Transition from amorphous Fe to polycrystalline body-centred-cubic Fe in Gd/Fe and Dy/Fe multilayered thin films

2002 J. Phys.: Condens. Matter 14 10033

(http://iopscience.iop.org/0953-8984/14/43/302)

INSTITUTE OF PHYSICS PUBLISHING JOURNAL OF PHYSICS: CONDENSED MATTER

J. Phys.: Condens. Matter **14** (2002) 10033–10040 PII: S0953-8984(02)37636-7

Transition from amorphous Fe to polycrystalline body-centred-cubic Fe in Gd/Fe and Dy/Fe multilayered thin films

K Engl, W Brunner and J Zweck

Universität Regensburg, Institut für Angewandte Physik, D-93040 Regensburg, Germany

E-mail: karl.engl@physik.uni-regensburg.de

Received 22 August 2002
Published 18 October 2002
Online at stacks.iop.org/JPhysCM/14/10033

Abstract

Rare-earth/iron multilayered thin films were magnetron sputtered to investigate the thickness-dependent transition from amorphous iron to polycrystalline body-centred-cubic iron. To characterize this transition it is necessary to get information about the average short-range order (SRO) in the multilayers. A unique technique for measuring this SRO is calculating pair distribution functions (PDFs) from reduced intensity functions by using high-energy electron diffraction in a 300 kV transmission electron microscope. With a maximum resolution in the PDFs of 0.024 nm, this method offers a high sensitivity for the investigation of the SRO. Due to the planar probing characteristics of the experiment, one gets structure information on interfaces rather than from the bulk structure. A further advantage of this method is that no specimen preparation is necessary. Therefore preparation artefacts can be excluded.

1. Introduction

Rare-earth/iron (RE–Fe) multilayered thin films are of great interest in developing new materials for magneto-optical storage media, because they can show uniaxial magnetic anisotropy perpendicular to the film plane [1]. As a possible source of this perpendicular magnetic anisotropy (PMA), an anisotropic distribution of RE–Fe pairs at the interfaces has been suggested [2]. Two important parameters for the PMA are the crystallographic change from amorphous Fe to polycrystalline body-centred-cubic (bcc) Fe and the formation of an alloy at the RE–Fe interfaces. Determining the atomic short-range order (SRO) of the specimens yields valuable information on these parameters and can help one to further improve their physical properties.

The determination of the SRO is carried out by calculating pair distribution functions (PDFs) from diffraction intensities. This method for structure investigation is well established

for amorphous and polycrystalline materials [3]. Though this method is usually applied to spatially isotropic specimens, it is also possible to use it with multilayered thin films. On account of the layer structure, the films are not three-dimensionally isotropic. Following the idea of Brunner [4], high-energy electron diffraction with an exact orientation of the film planes perpendicular to the electron beam can solve this problem.

The main attention in this paper is focused on the transition from amorphous Fe to polycrystalline bcc Fe in Gd/Fe and Dy/Fe multilayered thin films. The PDF method not only allows one to distinguish between these two structures, but also gives the range of the SRO in the specimens.

2. Theoretical approach

As Brunner [4] showed, it is possible to calculate PDFs for multilayered thin films by orientating the film plane of the specimen exactly perpendicular to the electron beam. In this case we detect the $k_z = 0$ plane in reciprocal space. For high-energy electron diffraction in a 300 kV TEM the reduced intensity function in Cartesian coordinates is given by

$$i(k_x, k_y, 0) = \int_{-\infty}^{+\infty} \int_{-\infty}^{+\infty} [\mathcal{P}(x, y) - \rho_0] \exp(\mathrm{i}k_x x) \exp(\mathrm{i}k_y y)\, \mathrm{d}x\, \mathrm{d}y, \tag{1}$$

where ρ_0 is the average atom density in the sample and $\mathcal{P}(x, y)$ gives the (local) particle density—averaged along the z-direction—in the direction of $\vec{r} = (x, y)$.

With the electron beam perpendicular to the film plane the diffraction patterns of multilayered thin films which show isotropy in the film plane are radially symmetric. In cylindrical coordinates the reduced interference function is given by

$$i(k, \varphi) = \int_0^{2\pi} \int_0^{\infty} [\mathcal{P}(r, \vartheta) - \rho_0] \exp(\mathrm{i}kr \cos(\vartheta - \varphi)) r\, \mathrm{d}r\, \mathrm{d}\vartheta, \tag{2}$$

where $r = |\vec{r}|$ and $k = |\vec{k}|$ (wavenumber). The angles between the x- and y-components of $\vec{r}$ and $\vec{k}$ are described by ϑ and φ. With the electron beam perpendicular to the film plane, all specimens showed radially symmetric diffraction patterns. Therefore the reduced interference functions are identical for all directions and we can set the angle $\varphi = 0$.

In the same way the structure of the multilayers is isotropic in the film plane, so $\mathcal{P}(r, \vartheta)$ does not depend on ϑ and can be written as $\mathcal{P}(r)$:

$$i(k, 0) = \int_0^{\infty} [\mathcal{P}(r) - \rho_0] \left[\int_0^{2\pi} \exp(\mathrm{i}kr \cos\vartheta)\, \mathrm{d}\vartheta \right] r\, \mathrm{d}r = 2\pi \int_0^{\infty} [\mathcal{P}(r) - \rho_0] \mathcal{J}_0(kr) r\, \mathrm{d}r, \tag{3}$$

where $\mathcal{J}_0(kr)$ is a zero-order Bessel function, which is generally defined as

$$\mathcal{J}_0(z) := \frac{1}{2\pi} \int_0^{2\pi} \exp(\mathrm{i}z \cos\beta)\, \mathrm{d}\beta \tag{4}$$

The inversion of the Fourier transform then gives the radially symmetric PDF:

$$\mathcal{P}(r) - \rho_0 = \frac{1}{2\pi} \int_0^{\infty} i(k) \mathcal{J}_0(kr) k\, \mathrm{d}k =: g(r). \tag{5}$$

The radially symmetric PDF $g(r)$ is obtained from reduced diffraction intensities $i(k)$. It contains information on the atomic SRO parallel to the film plane. The information which can be found from PDFs is mainly information about atomic neighbour distances and the average range of order. Each maximum in a PDF indicates a preferred neighbour distance corresponding to a coordination shell in crystalline materials. Since the PDF is basically the autocorrelation

Table 1. Sputter parameters used for different materials.

	Fe	Gd	Dy
Sputter power (W)	90	52	50
Sputter rate (nm s^{-1})	0.11	0.20	0.26
Target purity (%)	99.9	99.6	99.6

Table 2. Technical values for the sputter system.

Base pressure	$\leqslant 4 \times 10^{-7}$ Pa
Sputter gas	Argon 99.9999%
Ar pressure	0.8 Pa
Target–substrate distance	15 cm

function of the structure under investigation, it also reflects the average range of order (or mean crystallite sizes in polycrystalline materials). The envelope of an autocorrelation function of a particular structure approaches zero when the structure's dimensions are exceeded. This can in turn be used to estimate the average range of order from the point where the envelope of the PDF of a polycrystalline or amorphous structure approaches zero. This point is called r_0, the so-called 'cut-off radius' of PDFs, and can be taken as a measure for the average crystallite size parallel to the film plane. As the envelope function of the PDF approaches zero, uncorrelated 'data noise' becomes stronger, bearing no information. This 'data noise' is entirely due to computational rounding errors and noise in the reduced interference function. It is therefore a delicate but nonetheless achievable task to determine r_0, i.e. to decide where the 'real' information disappears and the noise component finally dominates.

Since the amorphous–polycrystalline distinction is not well defined, the range of the PDFs gives a rather precise measure for the range of crystalline order which allows one to detect a sharp transition from amorphous to polycrystalline Fe in RE–Fe multilayered thin films.

3. Specimens

As stated above, the scattering intensity for the $k_z = 0$ plane is detected. Therefore it is necessary to orientate the specimen precisely perpendicular to the electron beam. As this can be done easily with single-crystalline materials, we use silicon nitride (Si_3N_4) membranes on silicon wafer as substrates. At the edge of the Si_3N_4 membranes, the single-crystalline silicon is thin enough for us to get a spot diffraction pattern, which enables an exact orientation of the specimen perpendicular to the electron beam [4].

The multilayers were (magnetron) sputtered at room temperature with the sputter parameters given in table 1. The sputter system was operated at the constant parameters given in table 2.

The multilayers were sputtered on the silicon nitride substrates beginning with a layer of one of the RE metals. The multilayered thin films consist of eight periods of Gd/Fe or Dy/Fe. For the RE metals we used a constant single-layer thickness of about 3 nm. The iron layers were varied between 1.73 and 3.13 nm. All specimens were covered with an aluminium layer of approximately 3 nm to prevent oxidation. Figure 1 shows a schematic cross-section view of the multilayers.

The thickness of the multilayers was verified using x-ray fluorescence analysis (XFA) with a maximum error of 3%. As we get only the total thickness of the sputtered materials in the specimens from XFA, we calculate the (average) single-layer thickness by dividing the total thickness by the number of periods of the multilayered thin films.

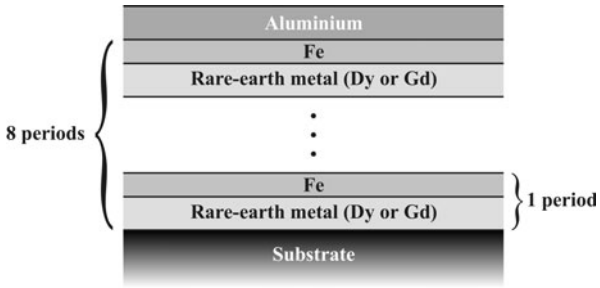

Figure 1. A cross-section view of the single-layer arrangement in the RE–Fe multilayered thin films.

4. Experiments

The experiments were carried out in a conventional transmission electron microscope (TEM) (Philips CM30) at the maximum electron energy of 300 keV. The diffraction patterns were recorded with a Gatan model 679 slow-scan CCD camera.

To get a reasonable resolution for the PDFs, the scattering intensity is measured from the centre of the diffraction pattern to a maximum scattering vector length $k_{max} \approx 320\ \mathrm{nm}^{-1}$ by recording a series of images. Then the radial resolution Δr of the PDFs—determined by the Airy distribution—is given by

$$\Delta r = 1.22\frac{2\pi}{k_{max}} = 0.024\ \mathrm{nm}. \tag{6}$$

The PDFs are measured as one-dimensional radial line scans from the diffraction intensities. As already mentioned, all specimens showed radially symmetric diffraction patterns. Therefore it is possible to minimize measuring errors by averaging the line scans over a circle sector with an angle of about 10° (since the diffraction patterns are recorded as a series of single images which have to be fitted to each other, the exact value of the angle depends on this fitting and the number of recorded images; the maximum value of the averaging angle is limited by the angular width of the outermost image). However, the averaging procedure results in a different weighting of the individual atomic distances (the angular extension $\Delta\varphi$ of a pixel depends on the distance r from zero, because the pixel size Δx is fixed), which can be corrected by multiplying the PDF $g(r)$ by r (centred stretching). This ensures that the ratio of the information related on one pixel of the CCD camera is restored. All PDFs given in this paper are presented as $rg(r)$ in arbitrary units.

5. Results

Before presenting the results of the investigation of the transition from amorphous iron to polycrystalline iron, we want to give some basic facts on the 'range' of PDFs.

5.1. Ranges of PDFs

Usually, thin films are not single crystals. Generally, they show amorphous-to-polycrystalline character. In the latter case they consist of arbitrarily orientated crystallites, while in the amorphous case a distinct SRO can be observed. In the PDFs, maxima represent preferred neighbour distances in the specimens. The cut-off radius r_0 defined by $g(r_0) \to 0$, i.e. where the envelope of the PDF approaches zero gradually, represents the average size of the crystallites (parallel to the film plane) in the specimens. With this value we have the possibility of making statements about the SRO in thin films as shown in figure 2.

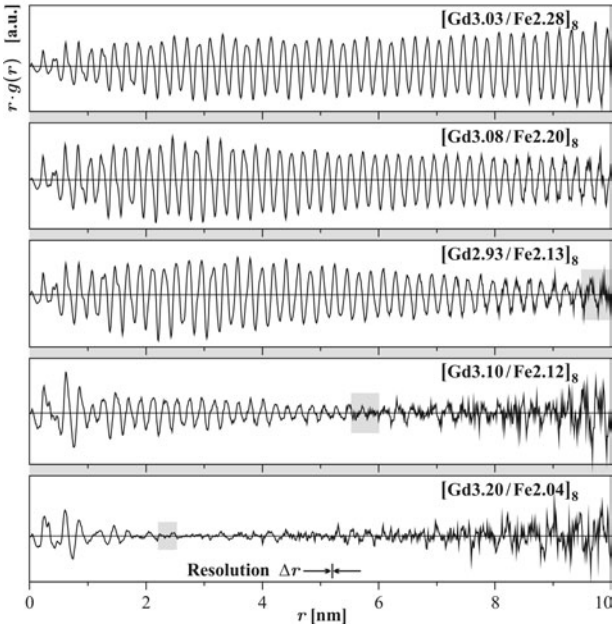

Figure 2. PDFs of different multilayered thin films with Gd layers of around 3 nm thickness and different Fe layer thicknesses. The area where noise starts to be significant is marked in grey. The range of the PDFs goes up with increasing iron single-layer thickness. The rise of the range from 2.4 nm to nearly 9 nm for a small increase of the iron layer thickness of only 0.09 nm is significant.

Comparison of the PDFs in figure 2 reveals a rapidly increasing range of the PDFs for only a small increase of the single-iron-layer thickness from bottom to top. At an iron thickness of 2.04 nm we get a range of about 2.4 nm. Increasing the single-layer thickness to 2.12 and 2.13 nm we get ranges of 5.2 and 9 nm, respectively. This is very significant, as a small increase of the thickness of only 0.09 nm results an enormous increase of the PDF ranges to around 9 nm. A further increase of the thickness results in ranges larger than 10 nm which are beyond reasonable computable values at the moment. But this is not the important point anyway, as the transition from amorphous iron to polycrystalline iron occurs obviously between 2.04 and 2.12 nm.

We tried to keep the average single-RE-layer thickness in all specimens constant at around 3 nm; it shows deviations between 2.93 and 3.20 nm. In PDFs of 'amorphous' specimens (the PDF ranges between 2.0 and 2.5 nm) no correlation between the deviation from 2.93 to 3.20 nm of the RE single-layer thickness and the range of the order could be found. This leads to the conclusion that the RE layers show the same amorphous structure over the given thickness range. In combination with an identification of the peaks of the PDFs with possible bcc iron interatomic distances, it was found that the range of the PDFs correlates with the structure of the iron layers which obviously depends on the thickness of the iron layers (see figure 3).

5.2. The transition from amorphous to polycrystalline iron

As stated above, the range of the PDFs is a measure for the mean size of the crystallites in the specimens parallel to the film plane. Figure 3 shows the range of the PDFs as a function of the single-iron-layer thickness in Gd/Fe multilayers.

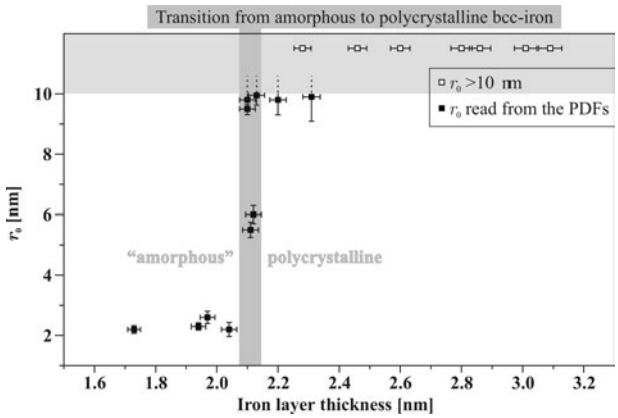

Figure 3. The relation between the single-iron-layer thickness and the range of the PDFs in Gd/Fe multilayers. The black squares show the range read directly from the PDFs; the white squares show ranges larger than 10 nm which cannot be calculated exactly at the moment. These marks are intended only to show that measurements have been performed for these iron layer thicknesses and the range is above 10 nm. The error bars relating to the layer thickness of the iron correspond to the precision of the XFA measurements. The variation of the cut-off radius is determined as shown in figure 2 from the areas marked in grey where noise starts to increase.

The sharp rise of the range of the PDFs from 2–3 to 9 nm and more at an iron single-layer thickness of 2.1 nm within a range of only 0.05 nm is significant. Also shown are specimens with ranges of more than 10 nm (white squares) which provide evidence for a polycrystalline order in the iron layers at a sufficient iron layer thickness.

The main result of these investigations of the range of PDFs of Gd/Fe multilayered thin films is the sharp transition from 'amorphous'[1] iron to polycrystalline bcc iron which occurs at a 'critical' single-layer thickness of iron of 2.1 nm. It is remarkable that a small increase of the iron layer thickness of only 0.05 nm leads to a rise of the range of more than 7 nm. As a consequence, the 'amorphous' SRO is more than doubled in range.

A similar behaviour can be observed in Dy/Fe multilayered thin films, as figure 4 shows, with the transition from amorphous iron to polycrystalline bcc iron. Here the transition occurs between 2.75 and 2.93 nm and leads from a range of less than 3 nm to a range of 9.5 nm. Though the transition is not as sharp as in Gd/Fe multilayers, the rise of the range of more than 6.5 nm for a difference of the single-layer thickness of iron of only 0.18 nm is quite remarkable.

A conventional explanation of this behaviour is a spontaneous crystallization of the iron layers when they reach a critical thickness [5]. This can be illustrated by TEM cross-section images (figure 5) of specimens with layers above the critical thickness of the iron layers. The areas of homogeneous contrast in the iron layers can be ascribed to crystallites with lateral extents of more than 10 nm, like those detected with the PDFs. According to this, the homogeneous contrast perpendicular to the layers gives evidence of a spontaneous crystallization of the iron layers after reaching the critical thickness. The TEM cross-section images show amorphous character for all RE layers. This gives evidence for there being no dependence of the range of the PDFs on the RE layer thickness.

[1] In the literature, thin films with crystallite sizes much smaller than 2.1 nm are often still called polycrystalline, but here it seems to be practical to use the expression 'amorphous' in connection with the critical iron layer thickness, as there is a sharp rise of the averaged size of the crystallites of more than a factor of 2 within a very small thickness variation, i.e. where a transition occurs between a mere SRO and an order of larger range.

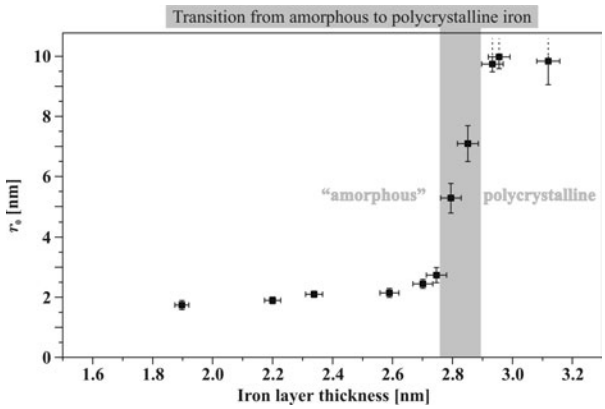

Figure 4. The transition from amorphous iron to polycrystalline bcc iron in Dy/Fe multilayers.

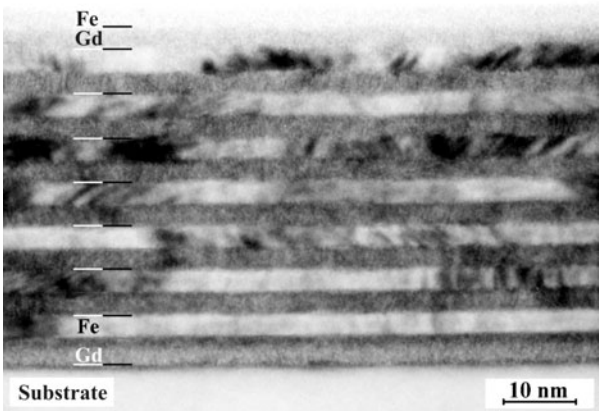

Figure 5. A cross-section image of a Gd/Fe multilayered thin film with 2.7 nm Gd layer and 3.1 nm Fe layer thicknesses. The Gd layers show amorphous character. The iron layers show homogeneous structures with lateral extents of some 10 nm. Together with the range of the PDFs, this gives evidence for a lateral crystallization of the iron layers after reaching the critical thickness of 2.1 nm.

5.3. Discussion

As has been shown, RE–iron multilayered thin films show a sharp transition from amorphous iron to polycrystalline bcc iron at a critical thickness of the iron layers. The transition occurs at about 2.1 nm in Gd/Fe multilayers and between 2.75 and 2.93 nm in Dy/Fe multilayers. TEM cross-section images provide evidence for a spontaneous crystallization of the iron layers above the critical thickness.

The difference in critical thickness of about 0.75 nm between Gd/Fe and Dy/Fe multilayers is assumed to be caused by the growing conditions of the iron and the sputter parameters. Brunner [6] showed, in his thesis, that the iron grows in the bcc modification with different textures depending on the RE materials. This means that Gd and Dy offer different growth conditions to the iron. The iron reaches a stable crystal structure at different values of the thickness depending on the RE metals, which leads to crystallization of the iron layers above the critical thickness.

Another reason could be found in the manufacturing parameters. Since the iron was sputtered at constant conditions for all specimens, the influence of the sputtering power has to be reduced to that for the RE materials. The RE targets were operated at similar powers of 50 W (Gd) and 52 W (Dy). For Gd we find a work function of 4.14 eV; for Dy the value for the work function is 3.04 eV [7]. These parameters result in different sputter rates of 0.20 nm s^{-1} for Gd and 0.26 nm s^{-1} for Dy. This can lead to a higher mean kinetic energy of the sputtered Dy atoms and also to a larger number of Dy atoms. Therefore a higher-energy transmission at the iron layers and an intermixing at the interfaces cannot be excluded.

6. Summary

We have shown that calculating PDFs from reduced intensity functions by using high-energy electron diffraction in a 300 kV TEM is a highly sensitive method for quantitative investigations of the SRO of amorphous-to-polycrystalline multilayer systems.

It was possible to precisely quantify a sharp transition from amorphous iron to polycrystalline bcc iron in Gd/Fe and Dy/Fe multilayered thin films depending on the RE metal. It was found that the transition occurs at different critical iron layer thicknesses of 2.1 nm in Gd/Fe and between 2.75 and 2.93 nm in Dy/Fe multilayers.

Since no specimen preparation was necessary, these results are virtually free of preparation artefacts.

References

[1] Stavrou E and Röll K 1999 *J. Appl. Phys.* **85** 5971
[2] Sato N and Habu K 1987 *J. Appl. Phys.* **61** 4287
[3] Cockayne D J H and McKenzie D R 1988 *Acta Crystallogr.* A **44** 870–8
[4] Brunner W 2001 *J. Phys.: Condens. Matter* **13** 2865–73
[5] Landes J, Sauer Ch, Kabius B and Zinn W 1991 *Phys. Rev.* B **44** 8342–5
[6] Brunner W 2002 *Beugungsexperimente und Paarverteilungsfunktionen zur Charakterisierung der Struktur von Seltenerdmetall/Eisen-Viellagenschichten im TEM* (Berlin: Logos)
[7] Kittel Ch 1996 *Einführung in Die Festkörperphysik 11 (Auflage)* (Munich: Oldenbourg)